NANO LETTERS

2006
Vol. 6, No. 2
258−262

Inelastic Transport through Molecules: Comparing First-Principles Calculations to Experiments

Magnus Paulsson,* Thomas Frederiksen, and Mads Brandbyge

MIC−Department of Micro and Nanotechnology, NanoDTU, Technical University of Denmark, Ørsteds Plads, Building 345E, DK-2800 Lyngby, Denmark

Received November 11, 2005; Revised Manuscript Received December 7, 2005

ABSTRACT

We present calculations of the elastic and inelastic conductance through three different hydrocarbon molecules connected to gold electrodes. Our method is based on a combination of the nonequilibrium Green's function method with density functional theory. Vibrational effects in these molecular junctions were previously investigated experimentally by Kushmerick et al. (*Nano Lett.* 2004, *4*, 639). Our results are in good agreement with the measurements and provide insights into (i) which vibrational modes are responsible for inelastic scattering, (ii) the width of the inelastic electron tunneling signals, and (iii) the mechanisms of heating and cooling of the vibrational modes induced by the coupling to the charge carriers.

The potential of molecular electronics has generated intense interest in electron transport through molecules. Measurements have been carried out by several research groups, see for example refs 1−4, and calculations have provided insight into the elastic and inelastic conductance.[5−13] However, no general consensus has been reached on whether the theoretical results match the experimental data. Several reasons have been proposed for the disagreements, ranging from limited knowledge of the geometrical arrangement of the molecules in experiments[14] to criticism of the often employed density functional theory (DFT).[15,16] It is especially appealing to describe transport using DFT since it is free of fitting parameters and computationally tractable even for large systems. It is therefore relevant to investigate what properties can be reasonably described by DFT, and to what extent.

Recent low-temperature measurements by Kushmerick et al.[1] have provided inelastic electron tunneling spectroscopy spectra (IETS) for three different hydrocarbon molecules (Figure 1) contacted by thin crossing gold wires. The IETS provide additional information compared to the often featureless elastic current−voltage ($I-V$) characteristics seen in experiments and theory. The purpose of our work is therefore to model the IETS using DFT and to critically compare with the experimental data.

Throughout this paper we utilize DFT combined with the nonequilibrium Green's function method (NEGF) to calculate (i) relaxed geometries, (ii) elastic transport properties, (iii) vibrational frequencies, (iv) coupling of vibrational modes to electrons (electron−phonon coupling), and (v) the IETS, here defined as

$$\mathrm{IETS} = \frac{\mathrm{d}^2 I/\mathrm{d}V^2}{\mathrm{d}I/\mathrm{d}V} \tag{1}$$

The methods we have developed to perform these calculations are summarized below with the full details to be published elsewhere.[17] Calculations of the IETS are carried out for the three molecules shown in Figure 1. The results are then discussed both in terms of the theoretical analysis and compared to the experimental results.

The SIESTA[18] and TranSIESTA[5] packages are used for the DFT calculations presented here.[19] To obtain plausible geometries of the molecules bonded to gold surfaces, geometry relaxation is performed for the atomic coordinates of the molecule as well as the surface gold atoms, i.e., the vibrational region in Figure 1. Periodic boundary conditions are utilized in the DFT calculations on unit cells consisting of one molecule together with 36 Au atoms (four layers of 3×3) to represent the Au(111) surfaces. The geometry optimization is repeated for different lengths of the unit cell in the direction perpendicular to the surface to find a (local) energy minimum.

Vibrational frequencies are calculated using finite differences. The dynamical matrix (Hessian) for the finite vibrational region (Figure 1) is found from the forces induced by displacing each of the atoms in all three directions by 0.02 Å. Calculated frequencies for small test systems, e.g., Au_2,

* Corresponding author: mpn@mic.dtu.dk.

10.1021/nl052224r CCC: $33.50
Published on Web 01/10/2006

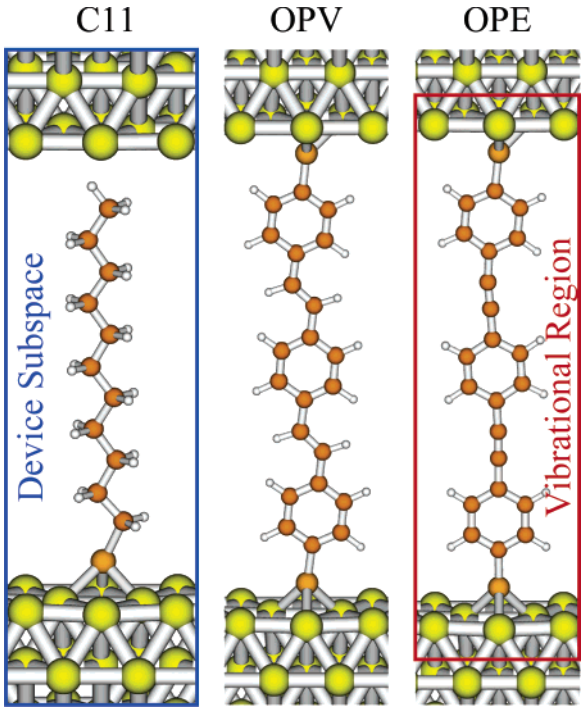

Figure 1. Relaxed geometries of the alkane chain (C11), oligophenylene vinylene (OPV), and oligophenylene ethynylene (OPE) studied in this work. The electron−phonon interaction is assumed to be limited to the device subspace and the molecular vibrations localized to the vibrational region as indicated in the figure.

C_2H_4, and C_2H_6, typically agree within a 5% error to experimental values. However, for larger molecules, the low-frequency vibrations show larger errors. For this reason low-frequency vibrations below 5 meV (compared to the important modes, see below) are removed from the calculations presented below.

The electron−phonon couplings ($M^{(\lambda)}$) are obtained from the vibrational modes ($\mathbf{v}^{(\lambda)}$) and the derivative of the Hamiltonian (H)[20]

$$M_{ij}^{(\lambda)} = \sum_{\alpha} \sqrt{\frac{\hbar}{2m_\alpha \omega_\lambda}} \left\langle i \left| \frac{\partial H}{\partial R_\alpha} \right| j \right\rangle v_\alpha^{(\lambda)} \qquad (2)$$

where $\{|i\rangle\}$ is the basis set, m_α is the mass of the atom corresponding to the nuclear coordinate R_α, and ω_λ is the angular frequency of mode λ. The derivatives of the Hamiltonian are calculated by a finite difference method.[21] To limit the range of the electron−phonon coupling, the interaction is assumed to be negligible outside the device subspace (Figure 1); i.e., the coupling is assumed to be limited to the molecule and the first two layers of gold atoms in the surface.

The current and consequently the IETS (eq 1) are calculated using the NEGF method in the lowest order expansion (LOE) approximation described in refs 9 and 21. This approximation relies on two assumptions: (i) expansion to lowest order in the electron−phonon coupling and (ii) constant density of states in the device and contacts close to the Fermi energy. For the molecules considered here, the first approximation is well justified since the electrons only interact weakly with vibrations; e.g., the experimental signal from inelastic scattering is weak. It is more difficult to rigorously justify the second approximation since the calculated transmission function varies around the Fermi energy for the molecules considered here. However, direct comparison of the inelastic signal in the full self-consistent Born approximation (SCBA) to the LOE reveals that the LOE works surprisingly well for molecules in the nonresonant limit;[17] i.e., differences in the calculated IETS are less than 10% for the test systems we examined.[22] The small errors may be rationalized by noting that the integrals approximated in the LOE approach resembles averages. If the average is well approximated by the functions at the Fermi energy, the LOE approximation is justified even if the integrands are energy dependent.

Our calculations include heating effects of the vibrational modes. To obtain the number of vibrational quanta in each mode, we impose the condition that the net power exchange between electrons and vibrational modes is zero for each vibration; i.e., the emission processes are balanced by creation of electron−hole pairs (electron−hole damping).[8,9] To simplify the discussion, we consider the low-temperature limit (our numerical results use the full temperature-dependent solution from ref 9) and solve for the number of vibrational quanta n_λ as a function of bias voltage (V)[23]

$$n_\lambda = \frac{\gamma_{\mathrm{em}}^{(\lambda)}}{\gamma_{\mathrm{eh}}^{(\lambda)}} \times \begin{cases} 0; & |\mathrm{eV}| < \hbar\omega_\lambda \\ |\mathrm{eV}/\hbar\omega_\lambda| - 1; & |\mathrm{eV}| \geq \hbar\omega_\lambda \end{cases} \qquad (3)$$

where $\gamma_{\mathrm{eh}}^{(\lambda)} = \omega_\lambda \mathrm{Tr}[M^{(\lambda)} A M^{(\lambda)} A]/\pi$ is the electron−hole damping rate and the vibration emission constant $\gamma_{\mathrm{em}}^{(\lambda)} = \omega_\lambda \mathrm{Tr}[M^{(\lambda)} A_1 M^{(\lambda)} A_2]/\pi$ is expressed in terms of the electron−phonon coupling ($M^{(\lambda)}$), the spectral densities resulting from the two contacts A_1 and A_2, and the elastic spectral function $A = A_1 + A_2$ (following the notation of ref 9). In deriving eq 3, we assume that there is no external damping of the vibrations. Any additional damping will simply decrease the number of vibrational quanta. However, coupling to the bulk phonons in the contacts for energies above the phonon bands (approximately 20 meV for gold) can only occur through nonharmonic means and is therefore likely to be weak.

In the following we present the calculated IETS for the three molecules using each molecule to highlight one concept at a time. Unless explicitly stated, the calculations include heating of the vibrational modes, broadening by a modulation voltage (see below), and use the device subspace and vibrational regions as shown in Figure 1. Since the calculated spectra are approximately symmetric (odd with bias) for all molecules, we only show the positive part of the IETS.

C11. The low-bias elastic conductance of the saturated alkanethiol molecule (C11), calculated using TranSIESTA, is $(1.6 \times 10^{-5})G_0 = 1.2$ nA/V per molecule where G_0 is the conductance quantum. For the C11 molecule, the low-bias conductance depends strongly on the electrode distance since the molecule is only bonded to one of the contacts. The measured conductance is approximately 17 nA/V.[1] Unfor-

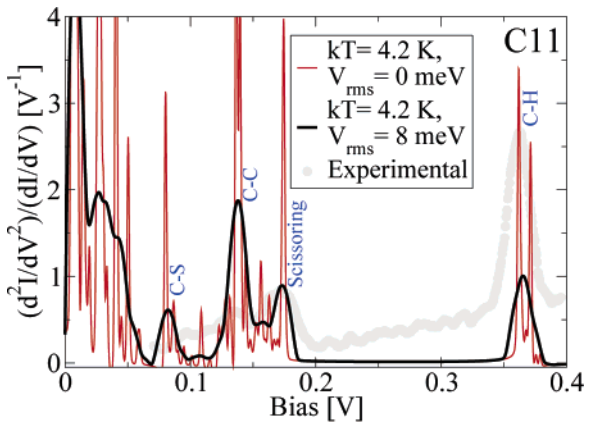

Figure 2. IETS for the C11 molecule broadened by thermal smearing (T = 4.2 K, thin red line) and additional broadening induced by the lock-in measurement technique (V_{rms} = 8 meV, thick black line). The experimental data originates from ref 1 (gray circles).

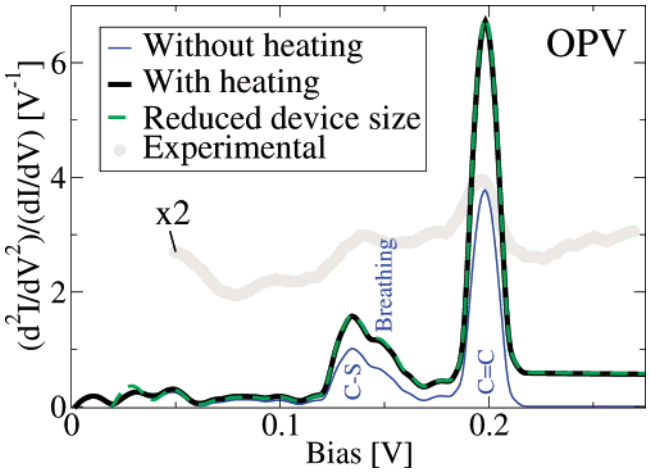

Figure 3. IETS for the OPV molecule. Inelastic signal without heating of the vibrational modes (thin blue line) and with heating (thick black line). The IETS calculated using a smaller device and vibrational region is also shown (dashed green line). Experimental data from ref 1 are scaled by a factor of 2 (gray circles).

tunately, we cannot compare these conductances since the measurements are performed on ensembles of molecules.

The calculated IETS is shown in Figure 2 using an electronic temperature of 4.2 K. For the low conductance systems studied here, each vibrational mode increases the conductance for a bias above the vibrational energy and gives a peak in the IETS.[9] The width of the peak is determined by thermal broadening (full width half-maximum (fwhm) = 5.4 $\times$ $k_B T$[9,24]). An additional broadening is introduced by the experimental lock-in measurement technique which adds a broadening fwhm = 1.7 $\times$ V_{rms} (in the d^2I/dV^2) where V_{rms} is the modulation voltage.[24] By broadening the IETS numerically using the same modulation voltage as in the experiments (V_{rms} = 8 meV), we obtain similar widths as in the experiment; see Figure 2.

OPV. The calculated low-bias conductance for the conjugated OPV molecule is $0.035G_0 = 2.8\ \mu$A/V per molecule and the IETS is shown in Figure 3. To verify that the device and vibrational regions used in the calculations are large enough to capture the IETS, calculations are carried out with

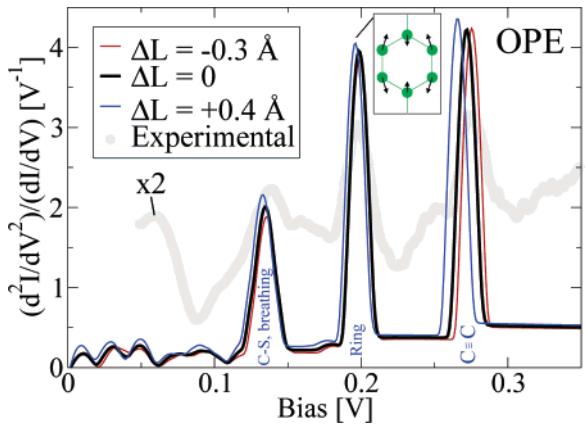

Figure 4. IETS for the OPE molecule for three different geometries corresponding to different electrode separations. Experimental data from ref 1 is scaled by a factor of 2 (gray circles).

these regions reduced in size. The smaller vibrational region consists of only the molecule while the device subspace is decreased to include the molecule and 2 $\times$ 9 gold atoms (one layer of each contact). The very small differences between IETS for the large and small regions confirm that we are using larger subspaces than necessary.

Heating enhances the IETS peaks due to stimulated emission and gives a constant shift beyond the vibrational energy, i.e., the conductance gathers a finite slope from the increase of vibrational quanta.[8] We can understand why the heating effect is important for the OPV and OPE molecules and negligible for the C11 molecule from eq 3. Due to Pauli blocking, an electron needs to traverse the device in order to emit a vibrational quantum. This is evident from the emission constant $\gamma_{em} \propto \mathrm{Tr}[MA_1MA_2]$ where the spectral densities resulting from the two contacts need to overlap. In contrast, absorption of vibrations is possible at all voltages and does not require that the electrons go through the device, $\gamma_{eh} \propto \mathrm{Tr}[MAMA]$. The saturated C11 molecule has a low-bias conductance 3 orders of magnitude smaller than those of the OPV and OPE molecules and consequently shows a much lower effect of heating. Further, it can be shown from the definitions of the emission constant and the electron−hole damping rate that $\gamma_{em}/\gamma_{eh} \leq 1/2$; i.e., *there exists an upper limit on the accumulated energy in a vibrational mode if the electron temperature is kept constant* ($n_\lambda \leq (|eV/\hbar\omega| - 1)/2$ for $|eV| > \hbar\omega$). This can be understood intuitively by noting that cooling of the device occurs by creation of electron−hole pairs in both contacts while the emission only takes place when electrons traverse the molecule.

OPE. The calculated low-bias conductance for the conjugated OPE is $0.021G_0 = 1.7\ \mu$A/V per molecule. The IETS is shown in Figure 4 for three slightly different electrode separations: (i) energy minimum, (ii) stretched by ΔL = 0.4 Å, and (iii) compressed by $\Delta L = -0.3$ Å. These changes in geometry give rise to only small changes in peak positions and heights in the IETS. This insensitivity to the exact geometry is instrumental in comparing experimental spectra to theoretical calculations.[25] If this was not the case, measurements would not be reproducible and calculations on plausible geometries useless. In addition, the peak heights

Table 1. Description of the Vibrational Modes Giving Rise to the Large IETS Signals for the Three Molecules[a]

	$\hbar\omega$ (meV)	γ_{em} (10^{10} s^{-1})	γ_{eh} (10^{10} s^{-1})	description
C11	41	6.1×10^{-4}	6.2	Au−S (+ C−C)
	80	5.5×10^{-4}	9.1	C−S
	136	16×10^{-4}	9.0	C−C
	140	11×10^{-4}	7.5	C−C
	174	10×10^{-4}	0.6	scissoring (+ C−C)
	361	14×10^{-4}	8.7	C−H last CH_3 group
	371	12×10^{-4}	2.9	C−H last CH_3 group
OPV	131	1.2	5.7	C−S
	133	1.5	5.6	C−S
	148	1.2	5.1	ring breathing
	193	2.5	11	ring[b] (+ C=C)
	198	15	37	ring[b] (+ C=C)
OPE	130	0.5	2.6	C−S
	131	1.0	4.8	C−S
	138	1.2	2.6	ring breathing
	198	4.0	12	ring[b]
	199	2.6	9.9	ring[b]
	271	7.1	16	C≡C
	274	2.5	7.1	C≡C

[a] Modes below 40 meV have been omitted in this table for the C11 molecule. [b] The ring mode is shown in the inset of Figure 4.

of the IETS are normalized with respect to the number of molecules, i.e., via the division by the conductance (eq 1). This justifies the direct comparison between calculations on individual plausible geometries and measurements on ensembles of molecules.

Comparison between the calculated and measured IETS shows that peak positions and widths are well described by our calculations. The relative heights of the different peaks agree for the OPE and OPV molecule while for the C11 molecule it does not, e.g., the C−H vibration peak around 360−370 meV is too small compared to the other vibrations. In addition, the measurements show a background signal[26] in the IETS, and the peak heights are smaller for the OPE and OPV molecule than in our calculations. One should note that any leakage current in the experiment would tend to decrease the peak heights. However, overall our calculations agree qualitatively with the experimental data by Kushmerick et al. and to the more approximate calculations by Troisi et al.[12] To understand the cause of the small discrepancies, more experimental evidence as well as calculations on additional molecular configurations is required.

The most influential vibrational modes for the IETS are listed in Table 1. It is interesting to note that in each of the molecules, only a few modes give the main contribution to the IETS. Although a detailed investigation of selection rules is outside the scope of this work, the calculations presented here suggest the following: (i) The C−S vibration gives a large signal and shifts in energy from 130 meV for the conjugated molecules to 80 meV for the saturated C11. (ii) The Au−S vibration is important for saturated molecules but does not affect conjugated molecules; see also footnote 25. (iii) Molecules containing benzene rings show two ring-based modes, "ring breathing" around 140 meV and "ring" at 200 meV (see inset in Figure 4) where the latter includes vibrations of the linking group (C=C) in the OPV molecule. (iv) Alkane-chains are either affected by vibrations coupling to the contacts (Au−S, C−S, or C−H) or involve the carbon chain (C−C). In addition to the clearly defined modes discussed above, many long-wavelength low-frequency modes (<40 meV) contribute to a large signal at low voltages for the C11 molecule. This resembles the low-bias anomaly seen in the experiment.

We have in this paper presented DFT-NEGF calculations describing inelastic scattering in three different molecules. We find (i) qualitative agreement with the measured IETS[1] for all three molecules without the use of fitting parameters, (ii) characterization of the vibrations responsible for inelastic scattering, and (iii) limitations on the accumulated energy in the vibrational modes from the heating and accompanying cooling effect of the vibrational modes by electrons. In view of the criticism of DFT-NEGF based conductance calculations, we note that the good agreement with experiments suggests that transport properties may be described by DFT. In particular, we believe the agreement of IETS relative peak heights (for the conjugated molecules) rules out gross errors in the position of the Fermi energy relative to the molecular resonances. However, we must also point out that due to the normalization of the IETS, there is no direct evidence that our DFT-NEGF method gives a correct broadening of the molecular levels by the contacts and thereby a correct low-bias conductance.

Acknowledgment. This work, as part of the European Science Foundation EUROCORES Program SASMEC, was supported by funds from the SNF and the EC sixth Framework Program. Computational resources were provided by the Danish Center for Scientific Computations (DCSC).

References

(1) Kushmerick, J.; Lazorcik, J.; Patterson, C.; Shashidhar, R.; Seferos, D.; Bazan, G. *Nano Lett.* **2004**, *4*, 639.
(2) Smit, R.; Noat, Y.; Untiedt, C.; Lang, N.; van Hemert, M.; van Ruitenbeek, J. *Nature* **2002**, *419*, 906.
(3) Reichert, J.; Weber, H. B.; Mayor, M.; von Löhneysen, H. *Appl. Phys. Lett.* **2003**, *82*, 4137.
(4) Xu, B. Q.; Tao, N. J. J. *Science* **2003**, *301*, 1221.
(5) Brandbyge, M.; Mozos, J.; Ordejon, P.; Taylor, J.; Stokbro, K. *Phys. Rev. B* **2002**, *65*, 165401.
(6) Lorente, N.; Persson, M.; Lauhon, L. J.; Ho, W. *Phys. Rev. Lett.* **2001**, *86*, 2593.
(7) Persson, M. *Philos. Trans. R. Soc. London* **2004**, *362*, 1173.
(8) Frederiksen, T.; Brandbyge, M.; Lorente, N.; Jauho, A. *Phys. Rev. Lett.* **2004**, *93*, 256601.
(9) Paulsson, M.; Frederiksen, T.; Brandbyge, M. *Phys. Rev. B* **2005**, *72*, 201101(R).
(10) Pecchia, A.; Di Carlo, A.; Gagliardi, A.; Sanna, S.; Frauenheim, T.; Gutierrez, R. *Nano Lett.* **2004**, *4*, 2109.
(11) Asai, Y. *Phys. Rev. Lett.* **2004**, *93*, 246102. Erratum *Phys. Rev. Lett.* **2005**, *94*, 099901(E).
(12) Troisi, A.; Ratner, M. A. *Phys. Rev. B* **2005**, *72*, 033408.
(13) Galperin, M.; Ratner, M.; Nitzan, A. *Nano Lett.* **2004**, *4*, 1605.
(14) Emberly, E. G.; Kirczenow, G. *Phys. Rev. Lett.* **2001**, *87*, 269701.
(15) Evers, F.; Weigend, F.; Koentopp, M. *Phys. Rev. B* **2004**, *69*, 235411.
(16) Toher, C.; Filippetti, A.; Sanvito, S.; Burke, K. *Phys. Rev. Lett.* **2005**, *95*, 146402.
(17) Frederiksen, T.; et al. In preparation.
(18) Soler, J.; Artacho, E.; Gale, J.; Garcia, A.; Junquera, J.; Ordejon, P.; Sanchez-Portal, D. *J. Phys. C* **2002**, *14*, 2745.

(19) We employ the PBE generalized gradient functional, the Γ-point approximation, double ζ-polarized (DZP) basis sets for the atoms of the molecule, single ζ-polarized (SZP) for the Au atoms, and a real space grid energy cutoff of 200 Ry.
(20) The derivatives of the Hamiltonian are corrected for the change in the basis set with displacement[21] and artificial direct coupling between the contacts caused by the periodic boundary conditions removed.
(21) Viljas, J. K.; Cuevas, J. C.; Pauly, F.; Häfner, M. *Phys. Rev. B* **2005**, *72*, 245415.
(22) The LOE approximations were confirmed to be quantitatively accurate by comparison to the inelastic signal from the full SCBA solution for the following two test systems: (i) a simple two-level model designed to mimic the HOMO−LUMO of a molecule and (ii) the OPE molecule described within DFT but with a minimal basis set, limited to the 10 most important vibrational modes, and a device and vibrational subspace only consisting of the molecule. Full SCBA calculations on larger systems are computationally infeasible. The SCBA calculations on the OPE molecule required approximately 100 CPU hours (P4 processors).
(23) Tikhodeev, S.; Ueba, H. *Surf. Sci.* **2005**, *587*, 25.
(24) Hansma, P. K. *Phys. Rep.* **1977**, *30*, 145.
(25) The relaxed geometries used in this work have the sulfur atom at the hollow position on the Au(111) surface. We cannot rule out that different Au−S bonding configurations will give qualitatively different inelastic signals for the Au−S vibration. However, in one test calculation, we found the on-top position to be unstable for the OPE molecule.
(26) The LOE approximation gives a bias independent elastic conductance. Retaining the bias dependence in the elastic conductance may contribute significantly to the background signal.

NL052224R